RESEARCH/REVIEW ARTICLE

Spatio-temporal variability of polynya dynamics and ice production in the Laptev Sea between the winters of 1979/80 and 2007/08

Sascha Willmes,[1] Susanne Adams,[1] David Schröder[2] & Günther Heinemann[1]

1 Department of Environmental Meteorology, University of Trier, Behringstr. 21, DE-54286 Trier, Germany
2 Centre for Polar Observation & Modelling, University College London, Gower Street, London WC1E 6BT, UK.

Keywords
Polynya dynamics; ice production; sea-ice remote sensing.

Correspondence
Sascha Willmes, Department of Environmental Meteorology, University of Trier, Behringstr. 21, DE-54286 Trier, Germany. E-mail: willmes@uni-trier.de

Abstract

Polynyas in the Laptev Sea are examined with respect to recurrence and interannual wintertime ice production. We use a polynya classification method based on passive microwave satellite data to derive daily polynya area from long-term sea-ice concentrations. This provides insight into the spatial and temporal variability of open-water and thin-ice regions on the Laptev Sea Shelf. Using thermal infrared satellite data to derive an empirical thin-ice distribution within the thickness range from 0 to 20 cm, we calculate daily average surface heat loss and the resulting wintertime ice formation within the Laptev Sea polynyas between 1979 and 2008 using reanalysis data supplied by the National Centers for Environmental Prediction, USA, as atmospheric forcing. Results indicate that previous studies significantly overestimate the contribution of polynyas to the ice production in the Laptev Sea. Average wintertime ice production in polynyas amounts to approximately 55 $km^3 \pm$ 27% and is mostly determined by the polynya area, wind speed and associated large-scale circulation patterns. No trend in ice production could be detected in the period from 1979/80 to 2007/08.

Coastal (wind-driven) flaw polynyas are nonlinear-shaped regions of open water and thin ice within a closed ice cover, formed by offshore winds advecting the pack ice away from the coast or fast-ice edge (Smith et al. 1990). The presence of a polynya provides a crucial link to a variety of processes at the ocean–atmosphere boundary and is associated with many feedback mechanisms. The atmospheric boundary layer is strongly modified when large amounts of heat are released from a polynya (Heinemann 2008; Ebner et al. 2011 [this volume]) and upper ocean stratification is significantly changed such that vertical mixing is supported when salt is released during ice formation (Martin & Cavalieri 1989; Dmitrenko et al. 2005; Williams et al. 2007). For seasons with available short-wave radiation, the combination with an enhanced upward flux of nutrients make polynyas some of the most biologically productive marine ecosystems (Arrigo & van Dijken 2004). Hence, recurrence and variability of polynyas as well as associated ice formation are key variables for monitoring the Arctic climate system. Flaw polynyas represent a characteristic feature in the coastal areas of the Arctic Ocean. Sixty-one recurring polynyas were identified in the Northern Hemisphere, differing significantly in size, shape and the amount of ice formed during the cold season (Smith et al. 1990; Barber & Massom 2007). As there is evidence for a shrinking Arctic sea-ice volume (Haas et al. 2008; Kwok et al. 2009), monitoring ice production within Arctic polynyas is crucial for assessing the balance between Arctic Ocean ice export, summer melt and winter freeze-up.

In the Laptev Sea during wintertime, off-shore components of the mean winds induce ice advection away from the coast, incorporating new ice into the Transpolar Drift and frequently causing areas of open water exceeding 100 km in width along the coastline and fast-ice edge (Dmitrenko et al. 2006). These recurring open-water areas are generally referred to as the Laptev Sea flaw

Citation: *Polar Research* 2011, *30*, 5971, doi: 10.3402/polar.v30i0.5971

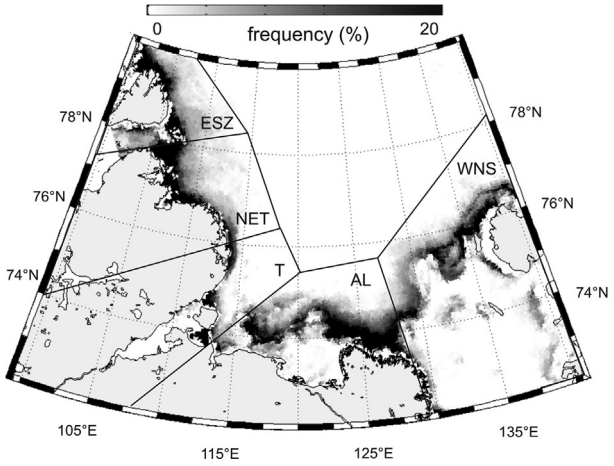

Fig. 1 Frequency of polynya occurrence during wintertime as derived from the Polynya Signature Simulation Method based on Advanced Microwave Scanning Radiometer–Earth Observing System microwave brightness temperatures, November–April, 2002–08. The following subareas were analysed: the eastern Severnaya Zemlya polynya (ESZ), the north-eastern Taimyr polynya (NET), the Taimyr polynya (T), the Anabar–Lena polynya (AL) and the western New Siberian polynya (WNS). Grid cell size is 6.25×6.25 km^2. A value of 20% means that on about 36 (out of 181) days between November and April a polynya was present in the respective grid cell. The maximum frequencies of occurrence are between 20% and 22% and are mostly found close to the fast-ice edge.

polynya (LSFP; Fig. 1) and represent locations where thermodynamic ice formation occurs almost continuously in response to a large heat loss from the ocean to the cold winter atmosphere. Hence, the LSFP is recognized as a strong ice producer, contributing directly to the ice volume transported with the Transpolar Drift (Reimnitz et al. 1994; Pfirman et al. 1997) and out of Fram Strait (Rigor & Colony 1997). Dethleff et al. (1998) estimate the annual ice production within the LSFP to amount to 258 km^3. The contribution of ice produced in the Laptev Sea to the entire Arctic sea-ice volume is subject to discussion in a wide range of studies (Zakharov 1966; Cavalieri & Martin 1994; Rigor & Colony 1997; Dmitrenko et al. 2009). The importance of the LSFP in terms of the volume of ice it produces relative to its small size is, however, well recognized (Dethleff et al. 1998; Bareiss & Görgen 2005).

A retrieval of long-term ice production is challenging for several reasons. First, the polynya area needs to be determined with a spatial and temporal resolution that is sufficient to capture the seasonal and regional dynamics of polynya events (Winsor & Björk 2000; Morales Maqueda et al. 2004; Tamura et al. 2008; Willmes et al. 2010). Second, heat loss over the polynya is to be calculated. This requires detailed information on the distribution and thickness of thin ice within in the polynya because even newly formed ice acts as an insulating layer between ocean and atmosphere, with the thickness of the ice determining its insulation capacity.

Sea-ice concentrations from microwave satellite data were used as a proxy for polynya area in several studies (Martin & Cavalieri 1989; Massom et al. 1998; Bareiss & Görgen 2005). Long-term sea-ice concentrations from scanning multichannel microwave radiometer (SMMR) and special sensor microwave imager (SSM/I) data provide a coarse resolution of only 25×25 km^2. Moreover, they are subject to an undetermined thin-ice bias (Kwok et al. 2007), which impedes a direct deduction of polynya area. A polynya classification approach known as the Polynya Signature Simulation Method (PSSM) based on satellite microwave brightness temperatures was suggested by Markus & Burns (1995) and successfully applied in other studies for a retrieval of polynya area (Kern 2008, 2009). The PSSM outperforms sea-ice concentration data in polynya area retrieval because it allows for an increased resolution of up to 5×5 km^2 and is not affected by a thin-ice bias.

Thin-ice thickness up to 0.2 m can be estimated based on passive microwave satellite data (Martin et al. 2004; Martin et al. 2005; Tamura et al. 2007). However, a case study for the Laptev Sea (Willmes et al. 2010) has shown that in narrow flaw leads and polynyas, coarse resolution satellite data provoke sources of error through mixed signals at the off- and onshore polynya edges. These problems and uncertainties raise the need for consistent input data of polynya area and thin-ice thickness when long-term ice production is to be determined from satellite records.

Here, we review wintertime (November–April) polynya dynamics in the Laptev Sea based on passive microwave and thermal infrared satellite data. From long-term sea-ice concentrations, we derive a consistent data set of daily polynya area. Hereafter, results are used together with thin-ice statistics and meteorological reanalysis to infer daily wintertime sea-ice production within the Laptev Sea polynyas, covering the period from 1979/80 to 2007/08.

Data and methods

Area of interest

The Laptev Sea covers the area between eastern Severnaya Zemlya in the west, the Lena Delta in the south and the New Siberian Islands in the east. We defined our regions of interest based on the subdivision of the LSFP by Bareiss & Görgen (2005) into five polynya regions: the

Citation: *Polar Research* 2011, *30*, 5971, doi: 10.3402/polar.v30i0.5971

eastern Severnaya Zemlya polynya (ESZ), the north-eastern Taimyr polynya (NET), the Taimyr polynya (T), the Anabar–Lena polynya (AL) and the western New Siberian polynya (WNS). Figure 1 presents the location of these areas within the Laptev Sea together with the relative wintertime polynya frequency as derived from PSSM (details below). Hereafter, the ESZ, NET and T polynyas will be referred to as the western Laptev Sea polynyas (WLS), while AL and WNS together represent the eastern Laptev Sea polynyas (ELS). This subdivision accounts for the different wind regimes maintaining these polynyas (WLS: west-/south-westerly winds, ELS: south-/south-easterly winds).

Polynya area from passive microwave data

In this study, we distinguish between (apparent) open-water area and polynya area. We use sea-ice concentrations from Nimbus-7 SMMR and DMSP SSM/I passive microwave data (Cavalieri et al. 1996; Meier et al. 2006), provided by the National Snow and Ice Data Center, USA, to estimate the wintertime (November–April) daily open-water area in the Laptev Sea between 1979/80 and 2007/08. The data set provides consistent sea-ice concentrations from October 1978 to the present. We started our investigations with the winter season of 1979/1980 since the meteorological reanalysis data used in this study (National Centers for Environmental Prediction [NCEP], USA, Reanalysis 2) are not available before 1979. The SMMR data (1978–07/1987) are available on an alternate-day basis only. Hence, temporal gaps were filled by linear interpolation between adjacent days in this period. The daily sea-ice area within each polynya box (see Fig. 1) was defined as the sum of all grid points that have an ice concentration of at least 15%. The apparent open-water area within each sub-area was subsequently derived by subtracting the sea-ice area from the total area of each polynya box.

Sea-ice concentration data are subject to uncertainties due to their large grid size (25×25 km^2), a bias of thin ice (Kwok et al. 2007) and the influence of leads. This impedes a direct determination of polynya area from the apparent open-water area as calculated from these data. Thus, the accurate polynya area (thin ice plus open water) was derived using the PSSM (Markus & Burns 1995; Arrigo & van Dijken 2004; Kern 2009), which provides a classification of thin-ice and open-water areas. The method is based on the sensitivity of passive-microwave polarization ratios (vertically minus horizontally polarized brightness temperature, normalized over their sum) to thin ice and open water. We used daily Advanced Microwave Scanning Radiometer–Earth Observing System (AMSR-E)/Aqua L2A Global Swath Spatially Resampled Brightness Temperatures data set (Ashcroft & Wentz 2008), available since 2002, to run the PSSM. The method combines the weaker atmospheric influence at 36 GHz (footprint size: 14×8 km^2) with the higher spatial resolution at 89 GHz (footprint size: 6×4 km^2). This is accomplished by applying a threshold to 89 GHz polarization ratio (PR89) maps and adjusting this threshold iteratively until the resulting classification agrees best with coincident 36 GHz polarization ratio maps. In previous studies PSSM was used with SSM/I 37 GHz and 85 GHz channels (footprint sizes: 37×28 km^2 and 15×13 km^2, respectively) after interpolating to a grid resolution of 12.5 km and 5 km, respectively, to obtain polynya maps at a resolution of 5×5 km^2. With the AMSR-E sensor, providing a smaller footprint, a similar resolution can be achieved without artificial gain of resolution and, hence, greater confidence.

The use of AMSR-E brightness temperatures within PSSM is possible since the antenna pattern of the sensor is comparable to SSM/I. Although a detailed quantitative comparison of AMSR-E and SSM/I derived PSSM polynya areas was not performed for this study, coincident data show that the frequency of small polynyas is underestimated by PSSM with SSM/I brightness temperatures, which is an effect of the relatively large footprint of the sensor.

Our implementation of the PSSM provides daily polynya maps with a spatial resolution of 6.25×6.25 km^2. According to Kern et al. (2007), the polynya area as derived by PSSM includes ice thickness of up to 0.25 m in the Antarctic. As salinity differences between different regions induce variable microwave properties of thin ice (Naoki et al. 2008), the upper ice thickness of a PSSM-derived polynya is subject to regional variability. A case study from the Laptev Sea shows that the detected polynya area in this region includes thin ice up to approximately 0.2 m (Willmes et al. 2010). An example is given in Fig. 2a, where the western New Siberian polynya is shown on 29 April 2008 in a moderate resolution imaging spectroradiometer (MODIS) visible channel image. Contour lines of the thermal ice thickness (0.2 m) and the PSSM polynya area indicate good agreement between these two parameters (Fig. 2b). As the abundance of ice thinner than the maximum PSSM ice thickness is necessary to carry out the intended determination of daily averaged heat loss (for an example, see Fig. 2c) and ice production, we use an empirical thickness distribution (see below). Applying this thickness distribution to the PSSM polynya area derived for the period from 2002 to 2008, we can take into account that the upper ice thickness limit in the polynya is subject

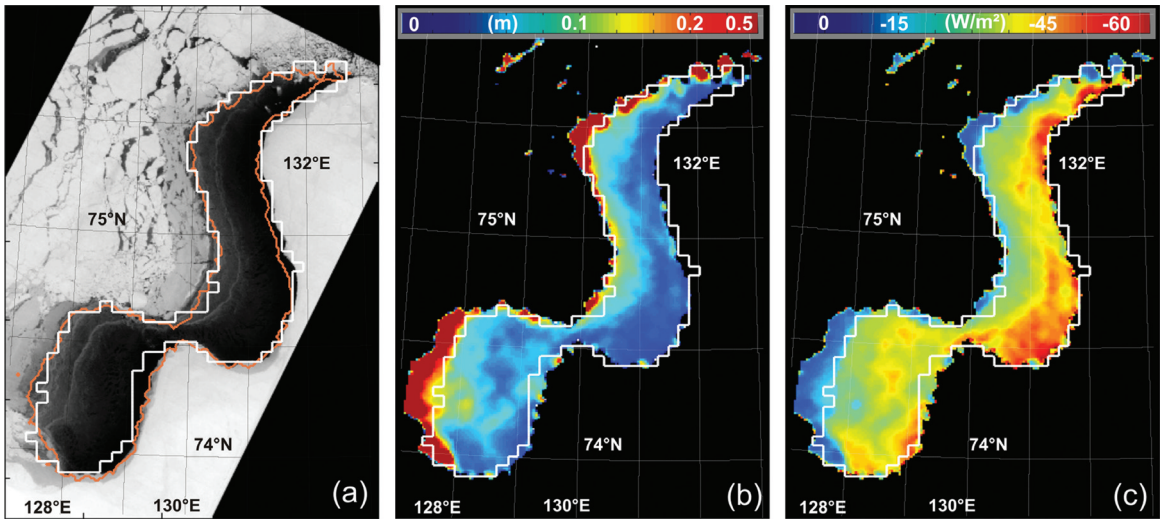

Fig. 2 (a) Moderate resolution imaging spectroradiometer (MODIS) visible channel (background) showing the WNS polynya on 29 April 2008 1100 UTC, the Polynya Signature Simulation Method (PSSM) polynya area (thick white line) and 0.2-m ice thickness contour line as derived from MODIS thermal infrared data (29 April 2008, 2100 UTC, orange line). (b) Thin-ice thickness (0–0.5 m) as derived from the thermal infrared data, values between 0.2 and 0.5 m are subsumed to increase colour contrast for values between 0 and 0.2 m. Thick white line indicates PSSM polynya area, as in (a). (c) Surface heat loss in W/m^2 for the presented snapshot in combination with daily averaged reanalysis data from the National Centers for Environmental Prediction (air temperature: −13°C, 10-m wind speed: 8 m s^{-1}).

to the uncertainty that arises from regionally differing microwave properties of thin ice.

Thin ice thickness from thermal infrared data

An empirical thin ice distribution for Laptev Sea polynyas was derived from Level 1B calibrated radiances (visible and thermal infrared) from the MODIS sensor, provided by the National Aeronautics and Space Administration (NASA), USA, Level 1 and Atmosphere Archive and Distribution System (LAADS). The entire MODIS data archive, covering the period from 2000 to date, was scanned for appropriate tiles applying automatic constraints such that the region of interest is sufficiently covered, clouds are not present and the image was acquired in the absence of shortwave radiation. The latter limitation is necessary because the thickness retrieval provides best results when albedo effects can be neglected. From the MODIS thermal infrared data that were obtained, surface temperatures were calculated following the split-window method of Riggs et al. (2003) for clear-sky regions as determined by the MODIS cloud mask product (MOD35). Hereafter, thermal ice thickness was inferred using the surface energy balance model suggested by Yu & Lindsay (2003) with the aid of daily NCEP/Department of Energy, USA, meteorological reanalysis data (Kanamitsu et al. 2002). The thickness retrieval is based on the assumption that the heat flux through the ice equals the total atmospheric heat flux (sum of net radiation, sensible and latent heat fluxes). The method yields good results for ice thicknesses below 0.5 m assuming further that vertical temperature profiles within the ice are linear and there is no snow on top of the ice. The relative accuracy of the thermal ice thickness was estimated to be about 20% (Drucker et al. 2003). The scanning of appropriate MODIS data yielded 336 appropriate tiles that were used to calculate the thermal ice thickness in the Laptev Sea. The number of obtained files was equally distributed over the months of November to April. A subsequent manual selection of valid polynya cases was necessary because some constraints could not be applied automatically. For example, parts of the polynya could be cloud-covered (most often through sea smoke over open water), while other parts are cloud-free, which would invalidate the actual thin ice distribution. Moreover, the area of a polynya could extend the area covered by a used swathe, such that only unrepresentative parts of the polynya are included. After such cases were deleted from the pre-selected MODIS tiles, 59 polynya cases (equally distributed over the months of November to April) were left to be used for the retrieval of thin-ice statistics.

A histogram in the value range from 0 to 0.5 m was calculated for each polynya event, before average histograms for the periods of November/December, January/February and March/April were derived with thickness class widths of 2 cm. Since only data from clear-sky events are taken into account, a systematic error might

Citation: *Polar Research* 2011, *30*, 5971, doi: 10.3402/polar.v30i0.5971

arise from the frequent occurrence of clouds over polynyas with a high fraction of open water. This uncertainty will be addressed using an "open-water scenario" within a sensitivity analysis for the ice production retrieval.

Ice production

The steps described above provided daily data of polynya area within each of the five polynya boxes from satellite microwave data in combination with a thin-ice climatology from MODIS thermal infrared images. Based on this, the daily averaged total atmospheric heat flux in each region could be determined using the NCEP variables 2-m air temperature, 10-m wind speed, sea-level pressure, specific humidity and downward shortwave radiation flux, which are provided at a spatial resolution of $2.5 \times 2.5^{\circ}$ Kanamitsu et al. 2002), each being interpolated to the polynya box centres. In this approach, the thin-ice climatology represents a tool to better approximate heat flux over a given polynya area with unknown ice thickness abundances. The total polynya area within each of the five boxes (Fig. 1) was subdivided into separate fractions for each thin-ice class, with each class being provided a characteristic albedo (Perovich 1996) and its average ice thickness (see the results for thin-ice distribution, below). Turbulent fluxes were determined from bulk equations for latent and sensible heat (Yu & Lindsay 2003). In our analysis, we applied a heat transfer coefficient of $C_H = 3 \times 10^{-3}$ used by Yu & Lindsay (2003), which is at the upper limit of the reported range. In addition, we performed a sensitivity analysis with a value of $C_H = 1 \times 10^{-3}$, which is at the lower limit (Schröder et al. 2003), to estimate its influence on the calculated ice production. Assuming that heat loss is entirely used for ice formation, new ice growth is determined by Eqn. 1, where Q_A is the daily averaged surface heat loss (W/m^2), ρ_i is the density of ice ($\rho_i = 900$ kg/m^3 adapted from Timco & Frederking [1995]) and L_i is the latent heat of fusion of sea ice ($L_i = 0.334$ MJ/kg):

$$\frac{\partial h}{\partial t} = Q_A / \rho_i L_i. \quad (1)$$

Results

Polynya dynamics

Open-water area from sea-ice concentrations can be used as a proxy for polynya area retrievals (Massom et al. 1998; Bareiss & Görgen 2005). Here we use the PSSM (Markus & Burns 1995; Kern et al. 2007) with AMSR-E microwave brightness temperatures to separate the polynya signal within sea-ice concentrations from disturbing influences causing open-water signatures (e.g., leads) and also to allow for a higher spatial resolution of polynya detection. A comparison of open-water area as derived from daily NASA Team sea-ice concentrations within the polynya boxes (see Fig. 1) and PSSM polynya area retrievals are presented in Fig. 3. The value distribution (daily averages, November–April 2002–08) shows that there is open water even if no polynya is present according to the PSSM applied to AMSR-E data. This "background open-water area" causes a non-linear relationship of the observed variables. At low open-water area and, hence, small polynyas, polynya area is not accurately represented by sea-ice concentrations. The non-linearity of the interrelation partly accounts for this bias. A polynomial model fitted to the relationship between PSSM polynya area and open-water area

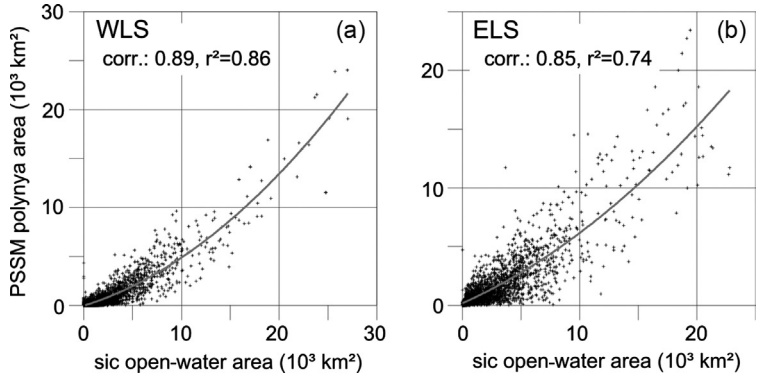

Fig. 3 Scatterplots of November–April 2002–08 daily averages of open-water area from National Aeronautics and Space Administration Team sea-ice concentrations (sic) and Polynya Signature Simulation Method (PSSM) polynya area for the (a) western (WSL) and (b) eastern Laptev Sea (ESL). Polynomial model fits are indicated by grey lines: (a) $-36.45 + 0.31x + 1.8 \times 10^{-5}x^2$ (root mean square error: 676.9 km^2); (b) $180.2 + 0.4x + 1.5 \times 10^{-5}x^2$ (root mean square error: 1417.2 km^2).

provides a coefficient of determination (r^2) of 0.86 and 0.74 for the WLS and ELS, respectively.

The presented polynomial fits were used to extend the high-resolution AMSR-E PSSM polynya area time series that is available from 2002 to 2008. The resulting data set provides the source of the subsequent analysis and represents the daily polynya area between 1979 and 2008. It is retrieved from daily open-water areas (as derived from SSM/I NASA Team sea-ice concentrations, 1979–2008; see Data and methods, above) with the aid of the polynomial models that were determined by a comparison with coincident values of polynya area from AMSR-E based PSSM (Fig. 3). Each of the five polynya regions was provided a separate polynomial model with these coefficients of determination (r^2): 0.87 (ESZ), 0.88 (NET), 0.80 (T), 0.85 (AL) and 0.67 (WNS). An investigation of case studies where polynya area was coincidently derived from MODIS-based thin ice thickness data indicates that the extended PSSM polynya area data set has an accuracy of $\pm 20\%$. This accuracy falls below the PSSM accuracy itself since it also includes ambiguities in the sea-ice concentration data that were used.

Hovmoeller diagrams of the obtained daily wintertime polynya area are presented in Fig. 4. It is revealed that during winter, early November shows the largest polynya area on average. This feature has strengthened during the last 10 years, indicating an effect of delayed fall freeze-up. The seasonal evolution of the polynya area is less pronounced up to the early 1990s compared to after that time. Afterwards, both early and late winter polynya areas start to increase while January and February polynya area decrease. Especially in the months of January to March, polynya area is on average significantly higher before 1990 than afterwards.

A comparison of the WLS and ELS (Fig. 4b, c) points out that the identified interannual changes of polynya area in the entire Laptev Sea are mostly due to the sea-ice variability in its western part.

Figure 5a, b shows average monthly polynya area values together with one standard deviation. A comparison of standard deviations for the WLS and the ELS indicates that the interannual variability of polynya area is remarkably smaller in the ELS in all months but April. However, in both regions the wintertime seasonal contrast (lower open-water area in mid-winter) appears to have strengthened during the observational period from 1979/80 to 2007/08 (Fig. 5c, d). January and February monthly averages in the ELS are characterized by significant negative trends, while positive trends are mainly found in November and April.

Some integrated parameters indicating long-term polynya dynamics were derived from the extended PSSM polynya area data set and are presented in Fig. 6. The

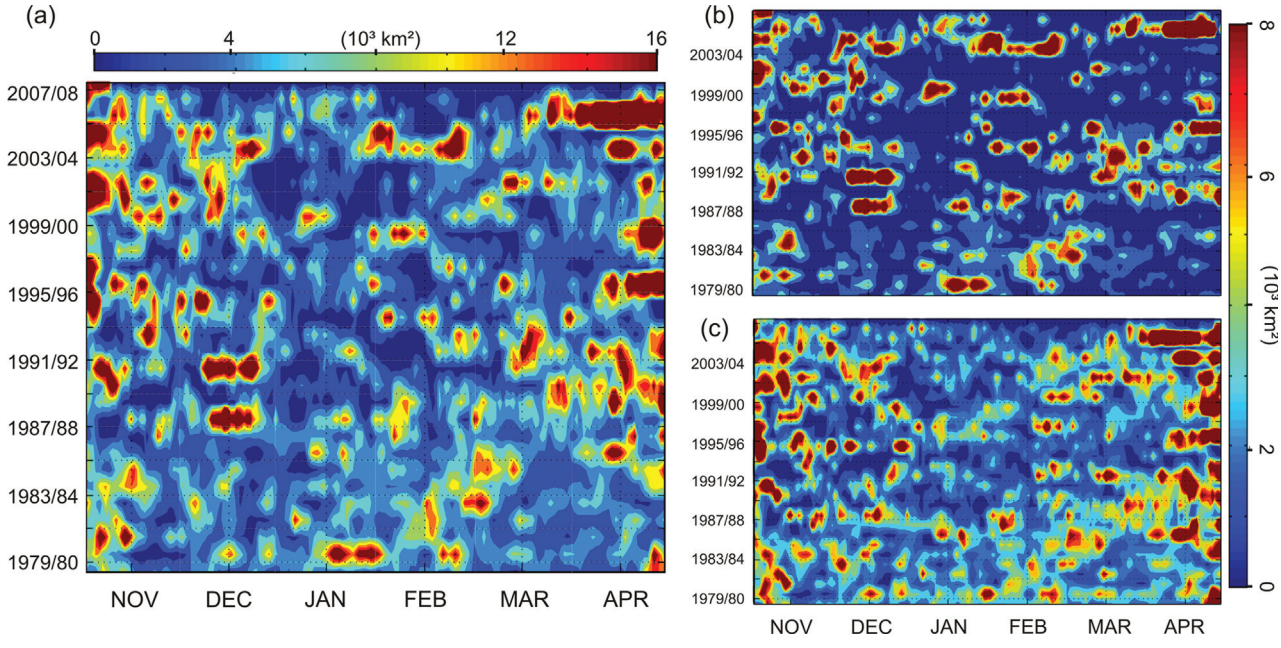

Fig. 4 Hovmoeller diagram of the daily polynya area (November–April 1979–2008): (a) entire Laptev Sea, (b) western Laptev Sea (eastern Severnaya Zemlya polynya, north-eastern Taimyr polynya and Taimyr polynya), and (c) eastern Laptev Sea (Anabar–Lena polynya and western New Siberian polynya), as derived from the extended Polynya Signature Simulation Method (PSSM) results.

Citation: *Polar Research* 2011, *30*, 5971, doi: 10.3402/polar.v30i0.5971

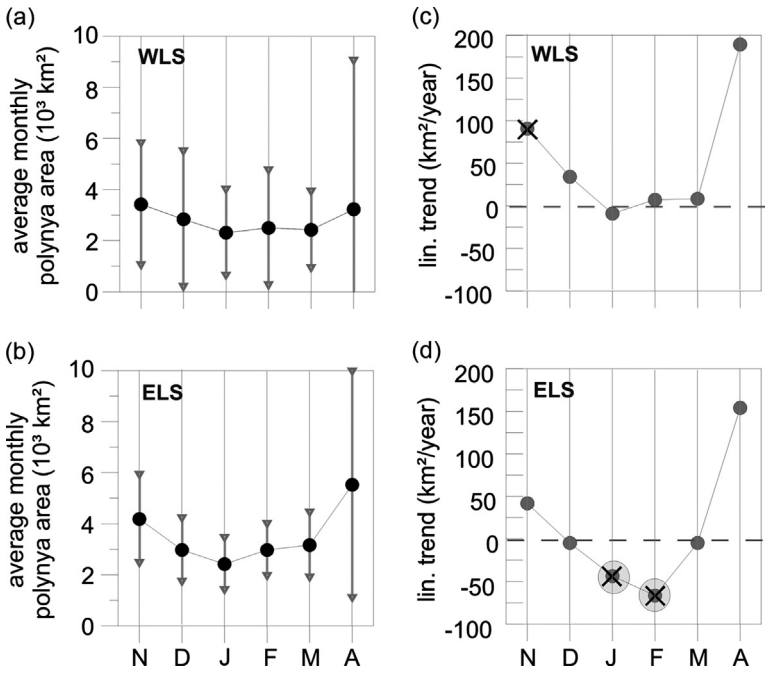

Fig. 5 Average wintertime evolution of polynya area from monthly means including one standard deviation for (a) the western Laptev Sea and (b) the eastern Laptev Sea; linear trends of monthly averages, 1979–2008 for (c) the western and (d) the eastern Laptev Sea. In (c) and (d), black crosses indicate significance at the 90% confidence level and grey circles indicate significance at the 95% confidence level.

accumulated wintertime polynya area in the WLS (Fig. 6a), representing the sum of daily polynya areas between November and April, is found to be on average 10% smaller than in the ELS (Fig. 6b). The winter of 2006/07 is outstanding within the 30-year time series in that the accumulated polynya area amounts to 1.2×10^6 km^2 in the WLS and approximately 1.0×10^6 km^2 in the ELS, while the long-term averages do not exceed 500 000 km^2 and 600 000 km^2, respectively. Similar patterns are observed in the seasonal maxima of daily polynya area (Fig. 6c, d). Daily polynya area maxima in the WLS are significantly lower in the period from 1979 to 1988 than in the following years.

This is not observed in the ELS. Strong maxima as seen in the winters of 1989/90 (WLS), 1999/2000 (ELS) and 2006/07 (ELS, WLS) result from very strong ice advection from the Laptev Sea into the central Arctic Ocean at the end of April (Zhang et al. 2008), while other large values can be explained with strong polynya activity throughout the entire winter. The frequency of strong polynya events seems to have increased since 1979.

Another east–west contrast of polynya dynamics in the Laptev Sea is shown in the zonal comparison of the number of days a polynya was present between November and April for different size classes (Fig. 6e, f). Polynyas larger than 2000 km^2 are less frequent during wintertime in the WLS (about 60 days on average) than in the ELS (about 90 days on average). In the WLS, the number of polynya days shows a significant positive linear trend for polynya size classes >5000 km^2 and $>10\,000$ km^2. In contrast, small polynyas (<5000 km^2) have become significantly less frequent in the ELS between 1979 and 2008, while the contribution of larger polynyas to all polynya events has increased slightly.

Figure 7a shows the coincidence of ELS and WLS daily polynya areas. The data distribution indicates that above an approximated threshold (ELS: 15 000 km^2, WLS: 25 000 km^2; see Fig. 7a), there is indication that a large polynya opening in the ELS implies the absence of a large polynya in the WLS. In contrast, the occurrence of a very large polynya in the WLS does not imply the absence of a polynya in the ELS as often. This pattern results from the fact that the Laptev Sea polynyas are wind-driven flaw polynyas and that the difference in orientation of the ELS and WLS coast or fast-ice fronts causes a different response to the current wind regime.

A histogram for polynya sizes is presented in Fig. 7b, c. The fraction of very small polynyas (<1000 km^2) makes the largest contribution (more than 40%) to the total number of polynya events in the WLS. Here, we have to take into account that, especially in the first histogram bin (0 to 1000 km^2), values are subject to uncertainties

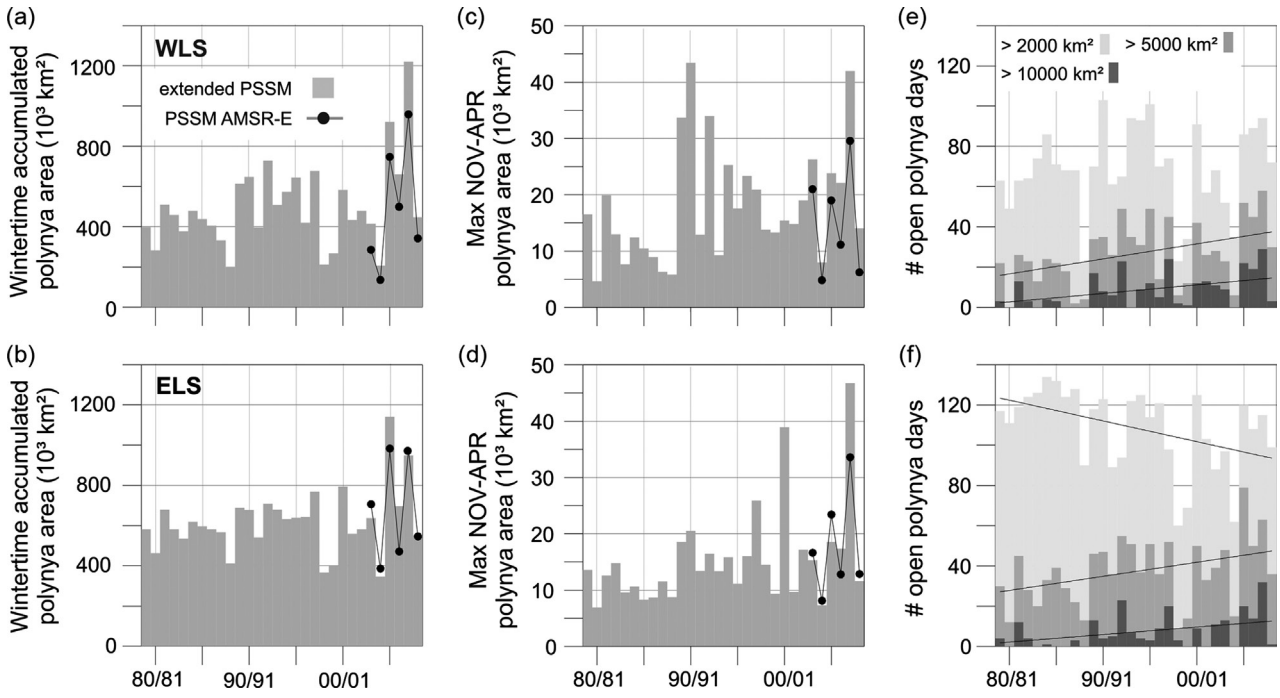

Fig. 6 Accumulated daily winter polynya area in (a) the western Laptev Sea and (b) the eastern Laptev Sea; seasonal maxima of daily polynya area in (c) the western and (d) the eastern Laptev Sea and the number of days with open polynya (area >2000 km^2, >5000 km^2 and $>10\,000$ km^2) in (e) the western and (f) the eastern Laptev Sea. Results are for the period November–April 1979–2008. Black lines indicate linear trends significant at the 95% confidence level.

due to the large grid size (625 km^2) of the NASA Team sea-ice concentrations that were used. Nevertheless, the histogram indicates that the probability density function for the polynya area is less steep in the ELS, where especially polynyas with a size between 2000 km^2 and 5000 km^2 are more frequent than in the WLS.

Thin ice distribution

The extended PSSM polynya time series provides valuable characteristics of the dynamics of areas with ice thickness of ≤ 0.2 m. The next step for an estimation of annual ice production within the Laptev Sea polynyas is to estimate the distribution and relative abundance of

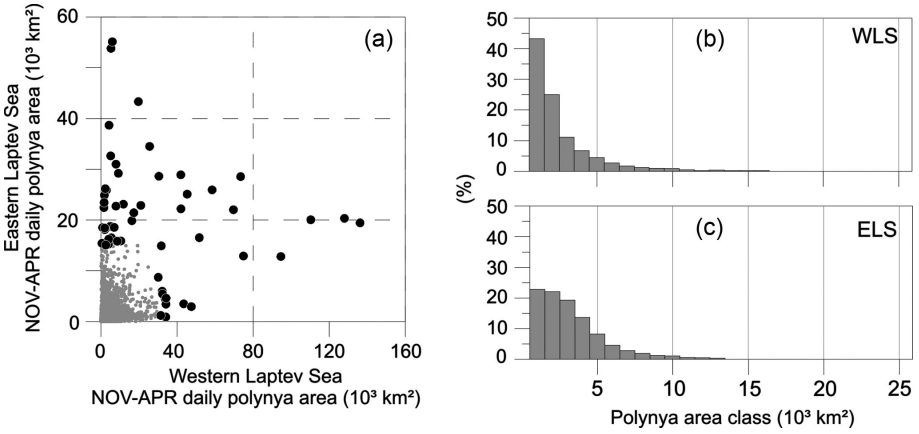

Fig. 7 (a) Scatterplot of daily polynya area in the western (WLS) vs. eastern Laptev Sea (ELS), black dots denoting values larger than 15 000 km^2 (ELS) and 35 000 km^2 (WLS); polynya area histogram for (b) the western and (c) the eastern Laptev Sea. Bin size is 1000 km^2, starting with (0 to 1000 km), x-axis value represents bin (x-1000 km^2 to x km^2).

Citation: *Polar Research* 2011, *30*, 5971, doi: 10.3402/polar.v30i0.5971

thin ice within the identified polynyas in order to calculate surface heat loss with the aid of meteorological data. As shown by Willmes et al. (2010), microwave proxies for the retrieval of thin-ice thickness suffer from their large footprint, provoking sources of error especially in narrow flaw polynyas. Here, we use high-resolution thin-ice thickness data derived from MODIS thermal infrared data to calculate an empirical thin-ice distribution (see Data and methods, above). The relative frequency of obtained thin-ice thickness values ≤ 0.2 m within the 59 MODIS swathes is presented in Fig. 8. The map clearly displays the average position of the recurring flaw polynyas in the ELS and WLS (compare Fig. 1). Please note that the values are not comparable with polynya frequencies in Fig. 1 since they only refer to the MODIS data subset while in Fig. 1, daily data from the entire investigation period are used.

A histogram for thin-ice thicknesses between 0 and 0.2 m is provided in Fig. 9. Ice thinner than 2 cm and open water contribute less, on average, than 2% to the total polynya area. This feature might be an effect of a bias that results from the fact that open-water regions are often a source of sea smoke. Consequently, these areas are more frequently flagged by the cloud mask and, hence, potentially under-represented in the thin-ice distribution. This needs to be accounted for using an "open-water scenario" in the ice-production estimation.

The area fraction of ice-thickness classes increases up to 7% for ice thicknesses between 2 and 4 cm and approximately half of the polynya is covered by ice of 12- to 20-cm thickness. The seasonal variation of this distribution lies within the standard deviation of each thickness class, although there is indication that the fraction of ice thicker than 12 cm decreases in March and April and average ice thickness decreases from 12.2 cm in November/December to 10.9 cm in March/April.

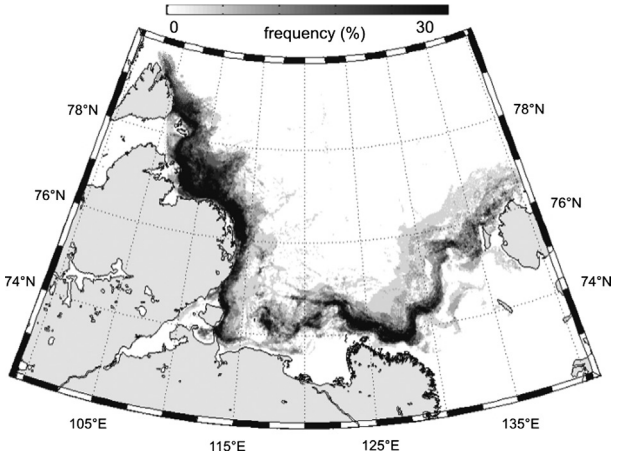

Fig. 8 Map of relative frequency of thin-ice thickness ≤ 0.2 m as derived from 59 selected moderate resolution imaging spectroradiometer (MODIS) thermal infrared image data, 2002–08 (compare to Fig. 1; for thin-ice thickness retrieval see Data and methods section).

Ice production

Daily averaged net surface heat loss and the associated ice production are calculated using Eqn. 1 based on daily data of polynya area (extended PSSM) within each of the five polynya boxes, assuming that the thin-ice thickness distribution within the polynya area can be described by the empirically derived thin-ice distribution presented in Fig. 9. Obviously, the empirical thin-ice distribution might be subject to notable uncertainties. Single polynya events probably significantly deviate from the average thin-ice distribution. Nevertheless, the thin-ice histogram provides a more detailed source for thin-ice thickness distributions than just assuming one average thin-ice thickness within each identified polynya. Our idea is that by calculating an "open-water scenario", which assumes that a polynya is entirely ice-free, we obtain an upper limit of ice production. The estimated total wintertime ice production between the winters of 1979/80 and 2007/08 is presented in Fig. 10. According to these results, 55.2 km^3 (standard deviation: 9.2 km^3) of ice are produced on average each winter within the polynyas of the Laptev Sea, partitioning to about 60% in the ELS and 40% in the WLS. The interannual maximum of ice production is found in 2004/05, when 73.3 km^3 were produced in the Laptev Sea polynyas. A minimum ice production of 35.7 km^3 occurred in 2003/04. We performed heat loss calculations with different modifications of input parameters to obtain a sensitivity analysis for the ice production retrieval (discussed below). We hereafter use the results obtained from the standard calculation (thin-ice thickness from histograms in Fig. 9, bars in Fig. 10) to further investigate the characteristics of ice production, keeping in mind that these results are subject to a potential bias in NCEP data, polynya area, heat loss calculations and thin-ice distributions.

The rates at which ice forms in the Laptev Sea polynya regions are presented in Fig. 11. There are no substantial regional differences either in averages or in maxima of daily ice formation rates (not shown). Maximum daily ice formation in the polynya area amounts to almost 20 cm, while the average between November and April is about 8 cm per day. However, there is indication for a seasonal contrast in maximum ice formation rates, with highest values in mid-winter and lowest values in late fall (Fig. 11a). This appears reasonable as air temperatures are coldest between January and March. In late April, the

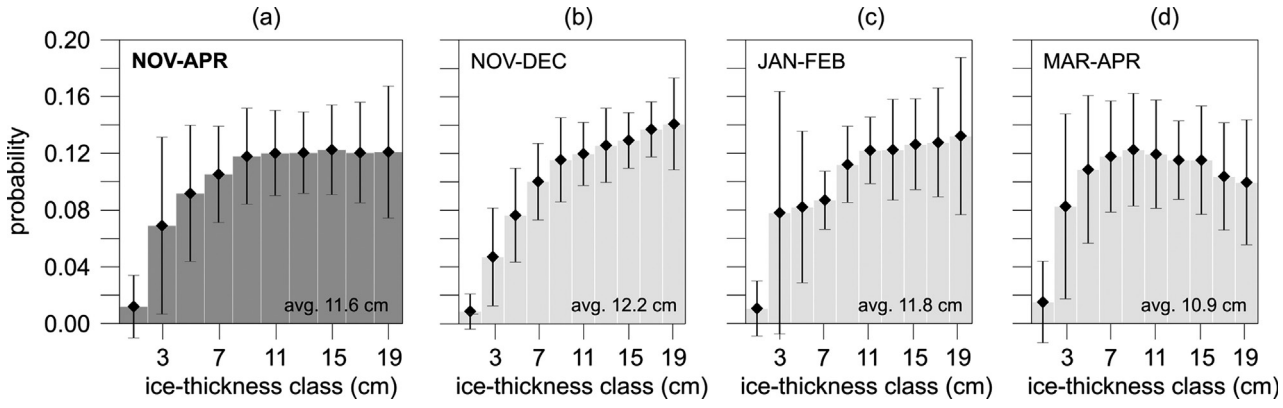

Fig. 9 Histograms for thin-ice thicknesses (a) averaged from November to April and for the months of (b) November–December, (c) January–February and (d) March–April. Error bars indicate one standard deviation.

total atmospheric heat flux might occasionally result in a surface heat gain due to the input of shortwave radiation.

The total volume of ice production is subject to regional differentiation (Fig. 11b). Most of the 55.2 km^3 of ice formed on average during wintertime originates from the AL polynya (17.4 km^3, 32%) while the T polynya (2.9 km^3, 5%) has the smallest average contribution to the ice production in the Laptev Sea.

The ELS polynyas (AL and WNS) are the source for 57% of the ice formed in the Laptev Sea polynya during the winter season and the highest regional ice production occurred in the WNS in the winter of 2004/05 (26.8 km^3). The WNS is also characterized by the largest interannual variability of wintertime ice production in terms of maximum and minimum value ($\pm$12 km^3), while the AL shows the highest standard deviation (4.4 km^3).

Assuming that ice formation in the entire Laptev Sea results in a regionally averaged first-year ice thickness of 1.4 m (Dethleff et al. 1998; Kwok et al. 2009), the total wintertime ice production should amount to 845 km^3

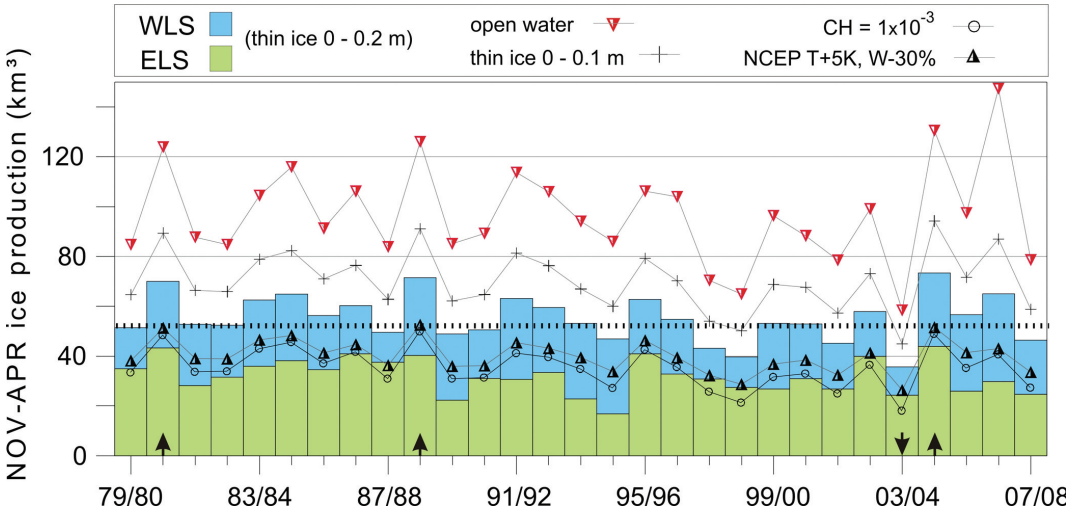

Fig. 10 Accumulated wintertime (November–April) ice production (km^3) in the Laptev Sea polynya areas. Bars indicate the standard retrieval with National Centers for Environmental Prediction (NCEP) data and an upper ice thickness of 0.20 m within the Polynya Signature Simulation Method area, split up into the eastern Laptev Sea (ELS, green) and western Laptev Sea (WLS, blue). The interannual average of 55.2 km^3 is shown by a black dotted line. Modified calculations (see the section on sensitivity analysis) are indicated by lines and symbols as follows: assuming an ''open-water scenario'' (grey line, red downward triangle), an upper ice thickness of 0.1 m within the polynya (grey line with crosses), a reduced heat transfer coefficient of $C_H = 1 \times 10^{-3}$ (grey line, open circles) and with modified NCEP data (2-m air temperature+5 K and 10-m wind speed −30%: grey line, upward triangles). Black arrows mark years with significant deviation from the long-term average (positive: upward arrow; negative: downward arrow) as estimated from the relative accuracy of the ice production retrieval (see the section on sensitivity analysis).

Citation: *Polar Research* 2011, *30*, 5971, doi: 10.3402/polar.v30i0.5971

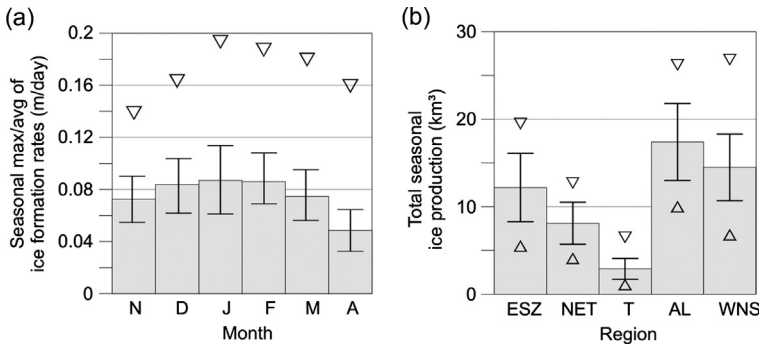

Fig. 11 (a) Average (bars), standard deviation (black vertical lines) and maximum (triangles) of seasonal ice formation rates (m/day) for the entire Laptev Sea polynya; (b) average (bars), standard deviation (black vertical lines), maximum and minimum (triangles) of total seasonal ice production (km^3) in each of the five polynya regions (eastern Severnaya Zemlya polynya [ESZ], north-eastern Taimyr polynya [NET], Taimyr polynya [T], Anabar–Lena polynya [AL] and western New Siberian polynya [WNS]) between November and April 1979/80–2007/08.

(considering the Laptev Sea covers an area of roughly 650 000 km^2), which would confirm results of Zakharov (1966). This value is also similar to what is suggested by Dmitrenko et al. (2009). Putting this into the context of our results, polynya ice production (55.2 km^3) accounts for only 8% of the total seasonal ice production and is significantly smaller than the figure of 30% in the study of Dethleff et al. (1998).

Sensitivity analysis

The interannual variability of the seasonal ice production as presented in Fig. 10 is subject to uncertainties in the derived thin-ice distribution, the obtained polynya area, the heat transfer coefficient that is used and the meteorological forcing data. The NCEP reanalysis data do not include modifications of the atmospheric boundary layer caused by polynyas, and thus tend to have biases in air temperature and wind speed in proximity of a polynya (see Ebner et al. 2011). The temperature bias is positive, while the wind speed bias can be positive or negative depending on the situation. If we assume a systematic bias in NCEP air temperatures of $-3^{\circ}C$ in case of a polynya, our values of ice production are consistently approximately 14% too high. Another systematic bias might arise from the used heat transfer coefficient ($C_H = 3 \times 10^{-3}$). Although this value was also used in previous studies (Yu & Lindsay 2003), Schröder et al. (2003) indicate that using a heat transfer coefficient of $C_H = 1.5 \times 10^{-3}$ would be more appropriate over thin sea ice. As shown in Fig. 10, a heat transfer coefficient of $C_H = 1 \times 10^{-3}$,which is at the lower limit of the values reported by Schröder et al. (2003), results in a systematic average decrease of 29% in the ice production that is obtained. Hence, assuming that the systematic errors reach this order of magnitude, our absolute values of seasonal ice production might be overestimated by +43% (NCEP air temperature and C_H bias combined), which means that these errors cannot close the gap between our results and those of previous estimates (e.g., Dethleff et al. 1998).

The interpretation of the interannual variability is impeded by non-systematic errors in the input variables. The effect of a given error range for each variable on the obtained ice production is given in Table 1. The assumed thin-ice distribution was varied based on the standard deviation of each ice-thickness class by assigning a larger/smaller contribution of thinner/thicker ice and vice versa. In doing so, the ice production varies by ±8%. The polynya area accuracy is estimated to be ±20%, which is estimated from a comparison with MODIS visible and thermal infrared data. The random error of the heat transfer coefficient is mostly due to variations in atmospheric stratification, while stable conditions are quite unlikely above a polynya.

Table 1 Estimated random errors of different input parameters and their effect on the calculation of daily ice production. The thin-ice distribution error is based on the standard deviations of each class as assigned in Fig. 9. The polynya area accuracy results from comparison with moderate resolution imaging spectroradiometer (MODIS) visible and thermal infrared data.

Variable	Thin-ice distribution	Polynya area	Heat transfer coefficient C_H	NCEP[a] T_{air}	NCEP[a] wind velocity
Random error	±SD	±20%	$\pm 0.5 \times 10^{-3}$	$\pm 2^{\circ}C$	±30%
△ Ice production	±8%	±20%	±6%	±9%	±12%

[a]National Centers for Environmental Prediction, USA

If we assume that the individual random error values of the resulting modifications in ice production presented in Table 1 follow a Gaussian error propagation, we can calculate the resulting random error for the accuracy of our ice production retrieval as $\pm 27\%$.

Consequently, the interannual variability remains significant when the deviation of annual ice production from the long-term average is more than approximately ± 15 km^3. This applies only to the winters of 1980/81, 1988/89, 2004/05 (ice production significantly high) and 2003/04 (ice production significantly low). During all other years, the deviation from the long-term means is below the estimated relative accuracy (compare Fig. 10).

Forcing mechanisms

The contribution of input parameters and large-scale atmospheric patterns to the seasonal and interannual variability of ice production is shown in Table 2. Most of the variability is explained by the polynya area. Correlation coefficients for daily polynya area and ice production are between 0.72 and 0.85 in all of the analysed regions. Correlation with daily averaged air temperature is positive, low and not significant. These positive correlations can be explained by the fact that low air temperatures occur mostly during strong inversions, which imply weak winds and, consequently, a small polynya area. Wind speed explains the wintertime ice-production variability significantly better with an average correlation coefficient of 0.46. Correlation with air temperature and wind speed was only calculated for cases when the prevailing wind direction favoured polynya opening (AL: 130–220°, WNS: 90–180°, ESZ/NET/T: 220–300°). The largest effect of the North Atlantic Oscillation (NAO) and the Arctic Oscillation (AO) is found in the WNS.

Here, inter-relationship with both indices is negative. In the AL, correlation is very weak and in the WLS (ESZ, NET, T), correlation is opposite to the WNS with an average correlation coefficient of 0.39 (AO) and 0.33 (NAO). The apparent weak response of ice production in the AL to the AO and NAO patterns might be a result of the fact that these atmospheric patterns in general favour easterly winds during positive phases and vice versa. Since the AL polynya is predominantly driven by southerly winds it responds more weakly to changes in AO and NAO. Annual wintertime average AO and NAO index values versus wintertime ice production are shown in Fig. 12 for the WLS and WNS. In the WLS, a negative AO/NAO index is more likely to result in lower ice production, while the opposite is true for the WNS in the eastern part of the Laptev Sea. In general, the correlation with AO is significant and somewhat larger than with NAO. In the WLS, 20 km^3 of ice were formed in one winter season when the AO was negative, while 26 km^3 of ice originated from this area during positive AO periods. In the WNS, wintertime ice production amounted to 16 km^3 (AO negative) and 12 km^3 (AO positive).

Discussion

According to Barber & Massom (2007), polynyas are "persistent and recurring regions of open water and/or thin ice or reduced ice concentration [...] that occur [...] at locations where a more consolidated and thicker ice cover would be climatologically expected" (p. 1). As such, this definition is hard to apply to a long-term satellite monitoring of a polynya. While open water is easy to distinguish from thick ice (e.g., Markus & Burns 1995), the thin-ice distribution within a polynya is more difficult to determine and the detectable upper thin-ice limit of the polynya area is subject to uncertainty. Using microwave properties of thin ice and open water for a polynya monitoring (for example, as in the PSSM) implies the effect of regional salinity variations, which impedes the determination of thresholds that are conferrable in space and time. A case study by Willmes et al. (2010) provided details on the microwave response to regional physical controls in the Laptev Sea. We assume that, on the basis of those results, the PSSM-derived

Table 2 Correlation of regional daily wintertime ice production (km^3) with daily averages of National Centers for Environmental Prediction 2-m air temperature (T2m), 10-m wind speed, extended Polynya Signature Simulation method polynya area; correlation of annual wintertime ice production vs. average wintertime Arctic Oscillation Index (AO; provided by the Climate Prediction Center, National Oceanic and Atmospheric Administration, USA) and average wintertime North Atlantic Oscillation Index (NAO; provided by Climate and Global Dynamics, National Center for Atmospheric Research, USA), 1979–2008. Underlined values are based on a significant linear relationship at the 90% confidence level, bold values are significant at the 95% level.

Correlation coefficients Nov–Apr 1979–2008	T2m	Wind speed 10 m	Polynya area	AO	NAO
Ice production					
Anabar–Lena Polynya	0.01	**0.52**	**0.72**	−0.19	−0.10
Western New Siberian polynya	0.21	**0.51**	**0.85**	**−0.46**	**−0.53**
Eastern Severnaya Zemlya polynya	0.19	**0.45**	**0.84**	**0.40**	0.36
North-eastern Taimyr polynya	0.20	**0.42**	**0.81**	**0.38**	0.33
Taimyr polynya	0.22	**0.36**	**0.84**	**0.40**	0.31

Citation: *Polar Research* 2011, *30*, 5971, doi: 10.3402/polar.v30i0.5971

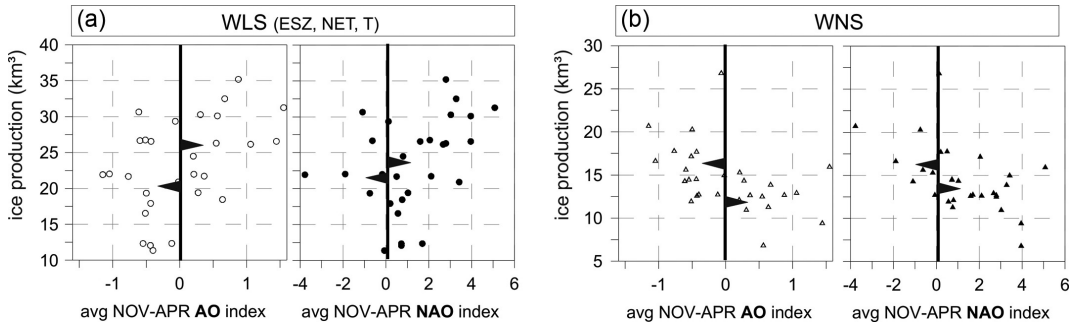

Fig. 12 Scatterplots of annual wintertime ice production (km^3) in (a) the western Laptev Sea (eastern Severnaya Zemlya, north-eastern Taimyr and Taimyr polynyas accumulated) and (b) western New Siberian polynya plotted against the average wintertime Arctic Oscillation (AO) and North Atlantic Oscillation (NAO) indices. Black triangles denote average ice production for positive and negative index values, respectively.

polynya area in our study includes open water and thin ice up to 0.2 m. Although thicker ice might also be part of a polynya according to the definition provided above, this study clearly addresses only areas below the 0.2-m thin-ice thickness threshold.

Wintertime ice production in the Laptev Sea and associated dense water formation were investigated in a wide range of studies using salinity measurements (Dmitrenko et al. 2009), wind-driven polynya models (Dethleff et al. 1998; Winsor & Björk 2000) or satellite sea-ice concentrations (Martin & Cavalieri 1989; Cavalieri & Martin 1994; Rigor & Colony 1997) to infer polynya area and associated ice production.

Dethleff et al. (1998) derived the amount of ice produced exclusively within the polynyas of the Laptev Sea. They obtain an ice production of 258 km^3 for the winter season of 1991/92, assuming a simple relationship between wind direction/wind speed and polynya area. For the same winter, our investigations yield an ice production of 63 km^3, which is 75% lower. This difference may be explained by the assumption of Dethleff et al. (1998) that thin ice is immediately removed from the polynya. This causes an overestimation of heat loss. But comparing their result with our "open-water scenario" (113.7 km^3 in 1991/92) still yields a difference of 50%. This may be attributed by differences in the retrieved polynya area, while we consider the satellite-based retrieval presented in this paper to exceed the accuracy of approaches that are simply based on NCEP wind speed and wind directions.

Winsor & Björk (2000) estimated the ice production in the Laptev Sea to amount to only 6 km^3 per winter season as an average between 1958 and 1997. Hence, their result, which is based on a wind-driven Arctic-wide polynya model, falls significantly behind our estimate even if we consider that the area they used for the Laptev Sea does not contain the ESZ, T and WNS. However, we also have to keep in mind that their study includes only open-water areas and does not account for surface heat loss and ice production over thin-ice areas. In this respect, we consider our results for the Laptev Sea to be more comprehensive in terms of the polynya definition provided above.

The net sea-ice production during wintertime was estimated to amount to 1000 ± 500 km^3 by Dmitrenko et al. (2009). This value represents the entire net ice production including autumn freeze-up over the entire shelf. Putting the results of Dmitrenko et al. (2009) in relation to the findings of this paper (55.2 km^3) we obtain a contribution of polynyas to the entire Laptev Sea ice production that is not higher than 4–11%. Dmitrenko et al. (2009) also describe a significant positive correlation of ice production with the AO index. Our results reveal that this interrelation is limited to the WLS polynyas (ESZ, NET, T), while in the WNS polynya ice production decreases during both positive AO and positive NAO phases.

Thin-ice thickness within polynyas was estimated from satellite microwave brightness temperatures in previous studies (Martin et al. 2004, 2005; Tamura et al. 2007). The Laptev Sea polynyas, however, are very narrow compared to the polynyas investigated in these studies. This complicates the use of low-resolution microwave data (Willmes et al. 2010), as was also noted by Martin et al. (2007) in the case of the Terra Nova Bay, Antarctica, and motivated us to use an empirical thin-ice distribution, which is based on high-resolution MODIS data. We therefore account for different ice-thickness classes within a polynya and in this way mitigate an overestimation of the net surface heat loss.

A key question arising from the observed interannual variability of ice production within polynyas is its impact on (a) the hydrography of the Arctic Ocean (through the formation of dense water) and (b) the general summer

sea-ice conditions in the Arctic. To address these questions, an updated Arctic-wide study of polynya dynamics and associated ice production would be beneficial. Within limitations, polynyas could act as a buffer of enhanced winter ice transport within the Transpolar Drift through an increase of ice formation when new ice is quickly advected out of the region of initial ice formation. On the other hand, strong polynya activity in combination with high advection rates probably favours large areas of thin ice to be incorporated into the Arctic Ocean and thereby might accelerate summer sea-ice melt. For example, in 2007 a lot of ice was advected from the Laptev Sea in April (Zhang et al. 2008), inducing enhanced new ice formation. However, the divergent drift patterns in late winter of this season might have caused a decrease in dynamic ice growth through compression and ridging and, thus, thinner ice.

The feedback mechanisms between polynya favouring atmospheric conditions (AO/NAO) and modifications in the cold Arctic halocline due to brine release still need to be identified and put into context with the interannual sea-ice variability in the Arctic Ocean. Another question that needs to be addressed in future studies is the contribution of leads within the pack ice to the total ice production.

Conclusions

Sea-ice concentration satellite data were used to derive daily wintertime open-water area in the Laptev Sea coastal region from 1979 to 2008. The results indicate an increased seasonality in open-water area that mostly arises from delayed autumn freeze-up and more open water during early spring in the western Laptev Sea.

The PSSM was used to correct for a bias in ice-concentration based polynya area estimates caused by (a) coarse resolution, (b) ice-concentration retrieval uncertainties over thin ice and (c) noise in high ice-concentration retrievals and to prepare an extended polynya area time series. The resulting polynya dynamics suggest an increased frequency of very large polynyas between 1979 and 2008.

Applying an empirical average wintertime thin ice thickness distribution from MODIS thermal infrared data to the polynya area, daily total atmospheric heat loss was calculated with the aid of meteorological reanalysis data. This approach yields an average wintertime ice production of $55.2\,km^3 \pm 27\%$ in the Laptev Sea polynyas and the absence of a significant trend in the period from 1979 to 2008. Regional differentiation in ice growth rates is negligible and amounts to a maximum of 20 cm per day. The influence of the AO pattern on ice production is opposed in the western and eastern Laptev Sea and is not documented at all in the Anabar–Lena polynya. This study suggests that polynya area is the dominant factor in determining the volume of ice that is produced.

Our investigations show that most of the previous studies significantly overestimate wintertime sea-ice production within the Laptev Sea polynyas. We suggest that this is mostly due to an overestimation in polynya area. Moreover, the distribution and abundance of thin ice are crucial for an accurate estimation of heat fluxes over the polynya.

Acknowledgements

We acknowledge that the constructive comments of two anonymous reviewers helped to improve our manuscript significantly. We are also grateful to Stefan Kern and Thorsten Markus for contributing valuable information and discussions. Sea-ice concentrations and AMSR-E brightness temperature data were provided by the National Snow and Ice Data Center, Boulder, CO, USA. MODIS thermal infrared satellite data were acquired from NASA's Level 1 and LAADS and meteorological reanalysis data from the NCEP/DOE. This work is supported by the German Ministry for Education and Research under grant no. 0360639E. Collaboration with project partners of the System Laptev Sea interdisciplinary research programme (Alfred Wegener Institute, Bremerhaven, Germany; GEOMAR, Kiel, Germany) and Russian colleagues from the Arctic and Antarctic Research Institute and the Otto Schmidt Laboratory for Polar and Marine Research, St. Petersburg, Russia is kindly acknowledged.

References

Arrigo K.R. & van Dijken G.L. 2004. Annual changes in sea ice, chlorophyll a, and primary production in the Ross Sea, Antarctica. *Deep-Sea Research Part II 51*, 117–138.

Ashcroft P. & Wentz F. 2008. *AMSR-E/Aqua L2A global swath spatially-resampled brightness temperatures V001, 2002–2008*. Digital media. Boulder, CO: National Snow and Ice Data Center.

Barber D.G. & Massom R.A. 2007. The role of sea ice in Arctic and Antarctic polynyas. In W.O. Smith Jr. & D.G. Barber (eds.): *Polynyas: windows to the world*. Pp. 1–43. Amsterdam: Elsevier.

Bareiss J. & Görgen K. 2005. Spatial and temporal variability of sea ice in the Laptev Sea: analyses and review of satellite passive-microwave data and model results, 1979 to 2002. *Global and Planetary Change 48*, 28–54.

Citation: *Polar Research* 2011, *30*, 5971, doi: 10.3402/polar.v30i0.5971

Cavalieri D. & Martin S. 1994. The contribution of Alaskan, Siberian, and Canadian coastal polynyas to the cold halocline layer of the Arctic Ocean. *Journal of Geophysical Research—Oceans 99*, 18343–18362.

Cavalieri D., Parkinson C., Gloersen P. & Zwally H.J. 1996 (updated 2008). *Sea ice concentrations from Nimbus-7 SMMR and DMSP SSM/I passive microwave data, 1979–2008*. Digital media. Boulder, CO: National Snow and Ice Data Center.

Dethleff D., Loewe P. & Kleine E. 1998. The Laptev Sea flaw lead—detailed investigations on ice formation and export during 1991/1992 winter season. *Cold Regions Science and Technology 27*, 225–243.

Dmitrenko I.A., Kirillov S.A., Tremblay B., Bauch D. & Willmes S. 2009. Sea-ice production over the Laptev Sea Shelf inferred from historical summer-to-winter hydrographic observations of 1960s–1990s. *Geophysical Research Letters 36*, L13605, doi: 10.1029/2009GL038775.

Dmitrenko I.A., Polyakov I., Kirillov S., Timokhov L., Simmons H., Ivanov V. & Walsh D. 2006. Seasonal variability of Atlantic water on the continental slope of the Laptev Sea during 2002–2004. *Earth Planetary Science Letters 244*, 735–743.

Dmitrenko I.A., Tyshko K., Kirillov S., Hoelemann J., Eicken H. & Kassens H. 2005. Impact of flaw polynyas on the hydrography of the Laptev Sea. *Global and Planetary Change 48*, 9–27.

Drucker R., Martin S. & Moritz R. 2003. Observations of ice thickness and frazil ice in the St. Lawrence Island polynya from satellite imagery, upward looking sonar, and salinity/temperature moorings. *Journal of Geophysical Research—Oceans 108*, 3149. doi: 10.1029/2001JC001213.

Ebner L., Schröder D. & Heinemann, G. 2011. Impact of Laptev Sea flaw polynyas on the atmospheric boundary layer and ice production using idealized mesoscale simulations. *Polar Research 30*, 5971, doi: 10.3402/polar.v30i0.5971.

Haas C., Pfaffling A., Hendricks S., Rabenstein L., Etienne J.L. & Rigor I. 2008. Reduced ice thickness in Arctic transpolar drift favors rapid ice retreat. *Geophysical Research Letters 35*, L17501, doi: 10.1029/2008GL034457.

Heinemann G. 2008. The polar regions: a natural laboratory for boundary layer meteorology—a review. *Meteorologische Zeitschrift N.F. 17*, 589–601.

Kanamitsu M., Ebisuzaki W., Woollen J., Yang S.K., Hnilo J.J., Fiorino M. & Potter G.L. 2002. NCEP-DEO AMIP-II reanalysis (R-2). *Bulletin of the Atmospheric and Meteorological Society 83*, 1631–1643.

Kern S. 2008. Polynya area in the Kara Sea, Arctic, obtained with microwave radiometry for 1979–2003. *IEEE Geoscience and Remote Sensing Letters 5*, 171–175.

Kern S. 2009. Wintertime Antarctic coastal polynya area: 1992–2008. *Geophysical Research Letters 36*, L14501, doi: 10.1029/2009GL038062.

Kern S., Spreen G., Kaleschke L., De La Rosa S. & Heygster G. 2007. Polynya Signature Simulation Method polynya area in comparison to AMSR-E 89 GHz sea-ice concentrations in the Ross Sea and off the Adélie Coast, Antarctica, for 2002–2005: first results. *Annals of Glaciology 46*, 409–418.

Kwok R., Comiso J.C., Martin S. & Drucker R. 2007. Ross Sea polynyas: response of ice concentration retrievals to large areas of thin ice. *Journal of Geophysical Research—Oceans 112*, C03S21, doi: 10.1029/ 2006JC003967.

Kwok R., Cunningham G.F., Wensnahan M., Rigor I., Zwally H.J. & Yi D. 2009. Thinning and volume loss of the Arctic Ocean sea ice cover: 2003–2008. *Journal of Geophysical Research—Oceans 114*, C07005, doi: 10.1029/2009JC005312.

Markus T. & Burns B. 1995. A method to estimate subpixel-scale coastal polynyas with satellite passive microwave data. *Journal of Geophysical Research—Oceans 100*, 4473–4487.

Martin S. & Cavalieri D.J. 1989. Contributions of the Siberian shelf polynyas to the Arctic Ocean intermediate and deep water. *Journal of Geophysical Research—Oceans 94*, 12725–12738.

Martin S., Drucker R.S. & Kwok R. 2007. The areas and ice production of the western and central Ross Sea polynyas, 1992–2002, and their relation to the B-15 and C-19 iceberg events of 2000 and 2002. *Journal of Marine Systems 68*, 201–214.

Martin S., Drucker R., Kwok R. & Holt B. 2004. Estimation of the thin ice thickness and heat flux for the Chukchi Sea Alaskan coast polynya from Special Sensor Microwave/Imager data. *Journal of Geophysical Research 109—Oceans*, C10012, doi: 10.1029/2004JC002428.

Martin S., Drucker R., Kwok R & Holt B. 2005. Improvements in the estimates of ice thickness and production in the Chukchi Sea polynyas derived from AMSR-E. *Geophysical Research Letters 32*, L05505, doi: 10.1029/2004GL022013.

Massom R.A., Harris P.T., Michael K. & Potter M.J. 1998. The distribution and formative processes of latent-heat polynyas in east Antarctica. *Annals of Glaciology 27*, 420–426.

Meier W., Fetterer F., Knowles K., Savoie M. & Brodzik M.J. 2006 (updated quarterly). *Sea ice concentrations from Nimbus-7 SMMR and DMSP SSM/I passive microwave data, 01/2008 – 04/2008*. Digital media. Boulder, CO: National Snow and Ice Data Center.

Morales Maqueda M.A., Wilmot A.J. & Biggs N.R.T. 2004. Polynya dynamics: a review of observation and modelling. *Review of Geophysics 42*, 1–37.

Naoki K., Ukita J., Nishio F., Nakayama M., Comiso J.C. & Gasiewski A. 2008. Thin sea ice thickness as inferred from passive microwave and in situ observations. *Journal of Geophysical Research—Oceans 113*, C02S16, doi: 10.1029/2007JC004270.

Perovich D. 1996. *The optical properties of sea ice*. Hanover, NH: U.S. Army Cold Regions Research and Engineering Laboratory.

Pfirman S.L., Colony R., Nuernberg D., Eicken H. & Rigor I. 1997. Reconstructing the origin and trajectory of drifting Arctic sea ice. *Journal of Geophysical Research—Oceans 102*, 12575–12586.

Reimnitz E., Dethleff D. & Nuernberg D. 1994. Contrasts in Arctic shelf sea-ice regimes and some implications: Beaufort

Sea versus Laptev Sea. *Marine Geology 119*, 215–225.

Riggs G.A., Hall D.H. & Salomonson V.V. 2003. *MODIS sea ice products user guide*. Greenbelt, MD: Hydrological Sciences Branch, NASA Goddard Space Flight Center.

Rigor I.G. & Colony R. 1997. Sea ice production and transport of pollutants in the Laptev Sea, 1979–2003. *Science of the Total Environment 202*, 90–110.

Schröder D., Vihma T., Kerber A. & Brümmer B. 2003. On the parameterization of turbulent surface fluxes over heterogeneous sea ice surfaces. *Journal of Geophysical Research—Oceans 108*, 3195, doi: 10.1029/2002JC001385.

Smith S.D., Muench R.D. & Pease C.H. 1990. Polynyas and leads: an overview of physical processes and environment. *Journal of Geophysical Research—Oceans 95*, 9461–9479.

Tamura T., Ohshima K.I., Markus T., Cavalieri D.J., Nihashi S. & Hirasawa N. 2007. Estimation of thin ice thickness and detection of fast ice from SSM/I data in the Antarctic Ocean. *Journal of Atmospheric and Oceanic Technology 24*, 1757–1772.

Tamura T., Ohshima K.I. & Nihashi S. 2008. Mapping of sea ice production for Antarctic coastal polynyas. *Geophysical Research Letters 35*, L07606, doi: 10.1029/2007GL032903.

Timco G.W. & Frederking R.M.W. 1995. A review of sea ice density. *Cold Regions Science and Technology 24*, 1–6.

Williams W.J., Carmack E.C. & Ingram R.G. 2007. Physical oceanography of polynyas. In W.O. Smith Jr. & D.G. Barber (eds.): *Polynyas: windows to the world*. Amsterdam: Elsevier.

Willmes S., Krumpen T., Adams S., Rabenstein L., Haas C., Hoelemann J., Hendricks S. & Heinemann G. 2010. Cross-validation of polynya monitoring methods from multi-sensor satellite and airborne data: a case study for the Laptev Sea. *Canadian Journal of Remote Sensing 36, Suppl. 1*, S196–S210.

Winsor P. & Björk G. 2000. Polynya activity in the Artic Ocean from 1958 to 1997. *Journal of Geophysical Research—Oceans 105*, 8789–8803.

Yu Y. & Lindsay R.W. 2003. Comparison of thin ice thickness distributions derived from RADARSAT Geophysical Processor System and advanced very high resolution radiometer data sets. *Journal of Geophysical Research—Oceans 108*, 3387, doi: 10.1029/2002JC001319.

Zakharov V.F. 1966. The role of coastal polynyas in hydrological regime of the Laptev Sea. *Oceanology 6*, 1014–1022.

Zhang J., Lindsay R., Steele M. & Schweiger A. 2008. What drove the dramatic retreat of Arctic sea ice during summer 2007? *Geophysical Research Letters 35*, L11505, doi: 10.1029/2008GL034005.